Cancer Nano (2013) 4:27–37
DOI 10.1007/s12645-013-0035-6

ORIGINAL PAPER

Active targeting of HER2-positive breast cancer cells by Herceptin-functionalized organically modified silica nanoparticles

Vahid Shirshahi · Fereshteh Shamsipour · Amir Hassan Zarnani · Javad Verdi · Reza Saber

Received: 28 December 2012 / Accepted: 20 February 2013 / Published online: 27 March 2013

Abstract Normal micelle microemulsion method was utilized for fabrication of organically modified silica (ORMOSIL) nanoparticles. The void and dye-doped nanoparticles were synthesized in nonpolar core of two different surfactants including Aerosol OT and Tween 80. The nanoparticles were characterized using transmission electron microscopy, dynamic light scattering, and zeta potential analysis. Our results revealed that the type of surfactant molecules has a dramatic impact on the size and size distribution range, surface charge, and surface functionalization of the nanoparticles. The particles fabricated using Tween 80 had very smaller size with narrow size distribution and very lower amount of zeta potential. For specific delivery of functionalized nanoparticles to breast cancer cell line SKBR3, overexpressing human epidermal growth factor receptor 2 (HER2), both dye-doped nanoparticles fabricated with Aerosol OT or Tween 80, was conjugated to Herceptin. In vitro studies using fluorescent microscopy demonstrated that the surfactant used for preparation of the nanoparticles can affect the uptake of the particles by cells. The dye-doped functionalized ORMOSIL nanoparticles prepared with Aerosol OT showed better efficiency in the process of active targeting of HER2 receptor. Herceptin-functionalized ORMOSIL nanoparticles can be used for differentiation of HER2-positive from HER2-negative breast cancer cells or specific delivery of therapeutic and diagnostic agents and also other nanoparticles such as magnetic nanoparticles and quantum dots to breast cancer cells.

Keywords ORMOSIL nanoparticles · Silica nanoparticles · Active targeting · Surface functionalization · Breast cancer

V. Shirshahi · R. Saber (✉)
Department of Medical Nanotechnology, School of Advanced Medical Technologies, Tehran University of Medical Sciences, Tehran, Iran
e-mail: rsaber@sina.tums.ac.ir

F. Shamsipour
Monoclonal Antibody Research Center, Avicenna Research Institute, ACECR, Tehran, Iran
e-mail: shamsipour@avicenna.ac.ir

A. H. Zarnani
Nanobiotechnology Research Center, Avicenna Research Institute, ACECR, Tehran, Iran
e-mail: zarnani25@yahoo.com

J. Verdi
Applied Cell Sciences in Medicine, Tissue Engineering Department, School of Advanced Medical Technologies, Tehran University of Medical Sciences, Tehran, Iran
e-mail: j_verdi@sina.tums.ac.ir

R. Saber
Research Center of Science and Technology in Medicine, RCSTIM, Tehran University of Medical Sciences, Tehran, Iran

1 Introduction

There are two various approaches for targeting tumor cells using nanoparticles: (1) passive targeting through the enhanced permeability and retention effect (Danhier et al. 2010) that takes advantage of special characteristics of tumors: angiogenesis, leaky vessels, poor lymphatic system, and results in passive accumulation of nanoparticles to tumor sites; (2) active targeting that takes advantage of overexpression of specific proteins and receptors in cancer cells, such as human epidermal receptor (HER) or transferrin and folate receptors, for enhanced delivery of targeting moiety-conjugated nanoparticles. This results in high local concentrations of nanoparticles on the surface of the cancer cells or internalization of nanoparticles into the cancer cells, depending on the type of selected biomoiety and its receptors. The second approach is very promising for

specific and selective delivery of therapeutic and diagnostic agents with better efficacy and lower toxicity (Byrne et al. 2008; Gu et al. 2007).

Among a family of four transmembrane epidermal growth factor receptor tyrosine kinases including HER1 to HER4 (Harries and Smith 2002), HER2 is highly overexpressed on 25 to 30 % of human breast cancer cells as well as some other human tumors including lung and ovarian carcinomas (Slamon et al. 1987; Witton et al. 2003). Hence, one of the most common approaches for breast cancer cells targeting has been using HER2-specific antibodies (Colombo et al. 2010). Herceptin or trastuzumab is a humanized monoclonal antibody against HER2 receptors approved as a drug by FDA in 1998 and is now used in metastatic breast tumors (Slamon et al. 2001).

Organically modified silica (ORMOSIL) nanoparticles are a kind of silica nanoparticles that are ultrasmall, monodisperse, spherical, mesoporous, and surface modified with an organosilane molecule such as (3-aminopropyl) triehoxysilane (APTES) (Yong et al. 2009; Qian et al. 2010). There are two main approaches for fabrication of silica nanoparticles including the Stöber method (Stober et al. 1968) as well as microemulsion processes either reverse micelle (Osseo-Asare and Arriagada 1990) or normal micelle (Roy et al. 2003). Typically, ORMOSIL nanoparticles are synthesized using normal micelle microemulsion procedure in which the self-assembled nanoreactors produced in an oil-in-water microemulsion system are used as surrounded microenvironments for hydrolysis and condensation of organosilane molecules such as Triethoxyvinylsilane (VTES) (Ciriminna et al. 2011; Yong et al. 2009). These nanoparticles have a number of advantages particularly for biomedical applications. Similar to other silica-based materials, ORMOSIL nanoparticles are inert and compatible with bioenvironments and biomolecules such as enzymes (Ciriminna et al. 2011). Since the particles have very small size range with narrow size distribution (10–50 nm), they are hidden from reticuloendothelial system, therefore capable for using in vivo (Roy et al. 2003). Moreover, these nanoparticles are transparent to light and very fascinating for applying in nanobiophotonics such as photodynamic therapy (Ohulchanskyy et al. 2007; Kim et al. 2007a, 2009) and optical bioimaging (Kim et al. 2007b; Kumar et al. 2008; Law et al. 2008; Qian et al. 2008; 2009; Wang et al. 2008). It is feasible to incorporate organic molecules such as organic dyes (Qian et al. 2008; Bagwe et al. 2004) and other nanoparticles such as quantum dots (Qian et al. 2009; Darbandi et al. 2005) or gold nanoparticles (Han et al. 2008) or even a combination of different nanoparticles (Bardhan et al. 2009; Viswanathan 2011) into the silica matrix. This strategy is a wise consideration to collect common beneficial characteristics of silica particles such as transparency, biocompatibility, and functionalizability with special properties of other nanoparticles such as photostability of quantum dots or thermal properties of gold nanoparticles.

Over the past decade, ORMOSIL nanoparticles have been developed by N. Prasad's group and other groups. They have applied Aerosol OT (AOT) and Tween 80 micellar systems in order to synthesis the nanoparticles (Roy et al. 2003; Kumar et al. 2008) and applied different targeting moieties for conjugation to the nanoparticles. To demonstrate the potential of ORMOSIL nanoparticles for bioconjugation, Kumar et al. functionalized the surface of the nanoparticles with various active groups and conjugated with different biomoieties and showed active targeting (Kumar et al. 2008). They also conjugated the nanoparticles with iodine-124, a positron emission tomographic imaging probe, and showed biodistribution of the nonspecific conjugated nanoparticles (Kumar et al. 2010). Qian et al. (2008) showed specific cellular uptake of amino group-functionalized ORMOSIL nanoparticles encapsulated with an organic dye and conjugated with apo-transferrin and folic acid in HeLa cells. Wang et al. used folate receptor functionalized ORMOSI nanoparticles entrapped a hydrophobic two-photon absorbing fluorenyl dye for two-photon fluorescence microscopy bioimaging in vitro. To confirm active targeting of nanoparticles, they applied HeLa cells and MG63 cells as high and low folate receptor expressing cell lines, respectively (Wang et al. 2008).

The surface modification of nanoparticles plays a critical role to provide novel properties and functionalities for the nanoparticles. In terms of ORMOSIL nanoparticles, the surface can be modified with various functional groups such as amine and carboxyl simply by replacing the organosilane precursor. The surface properties of silica particles plays a significant role in the interaction of the particles with bioenvironments (Nel et al. 2009) and determines the cellular uptake (Xia et al. 2009) and cytotoxicity (Nabeshi et al. 2011; Morishige et al. 2010) of the resulting particles. Moreover, the produced functional groups through surface functionalization can increase colloidal stability of the particles and can be utilized for conjugation to different biomoieties for targeting and specific gene/drug delivery to various cancerous cells (Klejbor et al. 2007; Bharali et al. 2005). The remained surfactant molecules on the surface of ORMOSIL nanoparticles synthesized by microemulsion method can affect their surface charge, surface functionalization, cellular uptake, and cytotoxicity. To solve the problem, several groups have tried to introduce novel methods for removing surfactant molecules from ultrasmall nanoparticles (under 50 nm) recently (Zhang et al. 2003; Salabat et al. 2008; Urata et al. 2009; Nazar et al. 2011; Hollamby et al. 2009; Sun et al. 2009).

In this work, we prepared ORMOSIL nanoparticles using normal micelle method and investigated the effect of the presence of different surfactants including AOT and Tween 80 on the surface charge of the nanoparticles and cellular uptake of dye-doped conjugated nanoparticles. The shape,

size, and surface charge of the resulting nanoparticles were characterized by transmission electron microscopy (TEM) and Zetasizer Nano. We also report the development of Herceptin-functionalized ORMOSIL nanoparticles as nanoplatforms for targeting HER2-positive breast cancer cells in vitro. Amino-active ORMOSIL nanoparticles synthesized by various surfactants were conjugated with Herceptin, and the platforms were utilized for active targeting of SKBR3, a breast cancerous cell line with highly expression of HER2 receptor, in vitro. For visualization and demonstration of the process of active targeting in vitro, we encapsulated Nile Red, an hydrophilic organic dye, in ORMOSIL nanoparticles, the dye becomes suitable for using in bioenvironments as an optical probe after encapsulation (Qian et al. 2008), and used optical imaging by fluorescence microscopy.

Herceptin-functionalized ORMOSIL nanoparticles are appropriate for labeling HER2-positive breast cancer cells and consequently differentiation of HER2-positive from HER2-negative breast cancers clinically. In addition, it can be loaded or linked with different therapeutic and diagnostic agents as well as other nanoparticles such as magnetic or gold nanoparticles or quantum dots and even a mixing of these particles and used as a vehicle for drug, gene, or nanoparticle delivery to breast cancer cells. Figure 1 shows a schematic view of the bioconjugation process of ORMOSIL nanoparticles with Herceptin.

2 Materials and methods

2.1 Materials

Surfactants AOT (98 %) and Tween 80 (viscous liquid), co-surfactants 1-butanol (99.8 %), ORMOSIL precursors VTES (97 %) and APTES (99 %), organic dye Nile Red (technical grade), and 1-ethyl-3-(3-dimethylaminopropyl) carbodiimide (EDC 98–100 %) were purchased from Sigma-Aldrich. All of the above chemicals were used without any additional purification unless noted. Breast cancer cell line SkBr3 was purchased from Pasteur Institute of Iran. All cells were incubated in RPMI-1640 medium (Sigma-Aldrich), supplemented with 10 % fetal bovine serum (FBS, Sigma-Aldrich), 100 units/ml penicillin–streptomycin, and incubated at 37 °C in a 95 % humidified atmosphere containing 5 % CO_2.

2.2 Synthesis of Nile Red-encapsulated amine-terminated ORMOSIL nanoparticles

ORMOSIL nanoparticles, with or without Nile Red, were synthesized based on the method described by Prasad's group. In separate experiments, the nanoparticles were synthesized in the nonpolar core of two different micellar systems including of AOT/1-butanol/DMSO and Tween 80/1-butanol/DMSO in deionized water. In a typical experiment, for each sample, the micelles were prepared by dissolving 0.2 g of Aerosol OT or Tween 80 and 300 μl of 1-butanol in 10 ml of deionized water using magnetic stirring, forming two different oil-in-water microemulsions. To each of the microemulsion systems, 100 μl DMSO was added; for preparing dye-doped nanoparticles, a 100 μl sample of clear solution of Nile Red in DMSO (5 mM) was added, by magnetic stirring, followed by addition 100 μl of neat VTES. The resulting solutions were stirred for about 1 h. Then, to initialize the polymerization reaction of the VTES precursor and make the nanoparticles amine-terminated, 15 μl neat APTES was added. In each solution, the polymerization reaction was completed within the precipitated nanoparticles by stirring for another 24 h at room temperature. For each solution of formed nanoparticles, dialysis against deionized water was used for purification of the nanoparticles using 12–14 kDa cutoff cellulose membrane for 2 days to remove surfactants AOT, Tween 80, co-surfactants 1-butanol, unreacted VTES and APTES, and free Nile Red. The remained surfactant molecules were removed by continuing dialyzing for 4, 6, and 8 days. Each dialyzed solution was then filtered through 0.22 μm

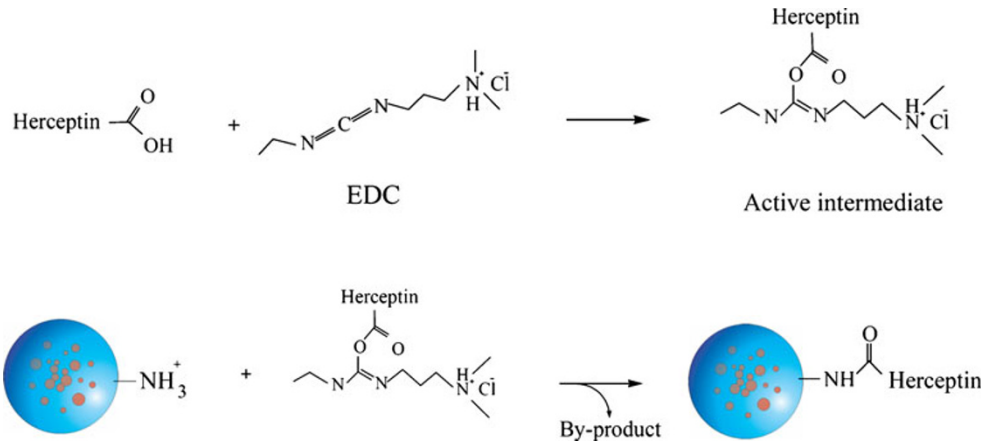

Fig. 1 The schematic view of the bioconjugation of Nile Red-encapsulated ORMOSIL nanoparticles with Herceptin

cutoff membrane filter and stored at 4 °C for later experiments. The nanoparticles prepared with AOT were named AOTORM and the particles prepared with Tween 80 named TWORM.

2.3 Characterization of the nanoparticles

2.3.1 Transmission electron microscopy and dynamic light scattering

To determine the morphology and the size of the resulting nanoparticles, transmission electron microscopy pictures were taken on a PHILIPS CM120 electron microscope operating at an accelerating voltage of 120 kV. A drop of the nanoparticles dispersed in water was put on a copper grid coated with Formvar solution. The pictures were taken after the grid dried.

The nanoparticles size was also determined by Zetasizer Nano (Malvern Instr, UK). The charge of the nanoparticles was quantified as zeta potential (Z.P) using a Zetasizer Nano (Malvern Instr, UK). Measurements were performed in deionized water with pH=8.

2.3.2 Zeta potential measurements

After the formation of the nanoparticles, Aerosol OT or Tween 80 surfactants and co-surfactant 1-butanol were removed gradually by dialysis the solution against double-distilled water in 12- to 14-kDa cutoff cellulose membranes then the dialyzed solutions were filtered through a 0.2-μm cutoff membrane filter and used for zeta potential measurements. The surface charge of nanoparticles was recorded before dialysis, after 2, 4, 6, and 8 days dialysis by using zeta potential measurements. In addition to nanoparticles, the zeta potential of AOT and Tween 80 micelles were recorded after micelle formation.

2.4 Bioconjugation of amine-terminated ORMOSIL nanoparticles with Herceptin

In separate experiments, the AOTORM and TWORM nanoparticles were conjugated to Herceptin (Roche, Switzerland) using a water-soluble carbodiimide, EDC. Herceptin powder was dialyzed in MES buffer (0.1 M, pH 6.5) and the concentration was determined with a UV–Visible spectrophotometer (Libra s22, Biochrom). To form linkages between carboxylates of Herceptin and primary amines of ORMOSIL nanoparticles, the reactions of EDC amide bond formation was used (Fig. 1). Because the effective pH for formation of EDC-mediated amide bond reaction is between pH4.5 and 7.5, we used MES buffer (0.1 M, pH 6.5) for conjugation reaction. EDC is more effective for activation of carboxyl groups; therefore, we added 50 μl EDC (0.1 M) to 200 μl Herceptin (2 mg/ml) solution in MES buffer. After 1 h incubation in room temperature, 1 ml ORMOSIL nanoparticle solution was added to active protein and incubated for 2 h at room temperature to allow the free amine groups of the nanoparticles to covalently bond to the carboxyl groups of Herceptin. Certain amounts of glycine were added to the solutions of conjugated nanoparticles to block remaining active groups. After purification, all samples were stored at 4 °C for additional cell experiments.

2.5 Cell culture and cellular imaging

SKBR3 cells, a breast cancer cell line with overexpression of HER2 receptors, were cultivated in RPMI 1640 media with 10 % FBS, 1 % penicillin, and 1 % streptomycin. One day before treatment with the nanoparticles, cells were seeded in eight-well glass slide (each well 3×10^4 cells).

During the treatment, the separate wells were incubated with 50 μl of different samples including dye-doped conjugated ORMOSIL (either AOTORM or TWORM) nanoparticles (2 mg/ml), dye-doped non-conjugated ORMOSIL (either AOTORM or TWORM) nanoparticles (2 mg/ml), Herceptin solution (10 μg/ml) followed by Sheep Anti Human IgG-FITC (0.2 μg/ml). After adding each sample, the cell incubation process lasted for 2 h at 37 °C in a humidified 5 % CO_2 atmosphere. Then, the cells were washed thrice with PBS buffer and directly imaged with a Fluorescence Microscopy (BX51, Olympus). The used excitation and emission wavelengths for fluorescent imaging were, respectively, 570 and 640 nm.

3 Results and discussion

3.1 Characterizations of ORMOSIL nanoparticles

ORMOSIL nanoparticles using normal micelle microemulsion formed by AOT or Tween 80 were synthesized with narrow size distributions and spherical shape, as shown by TEM images and dynamic light scattering (DLS) in Figs. 2 and 3, and named AOTORM and TWORM, respectively. Figure 2a shows TEM images of AOTORM nanoparticles with diameter around 25–50 nm; the particles have an average hydrodynamic diameter of 35 nm (Fig. 3b). Figure 2b shows that TWORM nanoparticles have a diameter of 15–20 nm and their average hydrodynamic diameter is 10.9 nm (Fig. 3d).

Normal microemulsion is a common method for synthesis of spherical and highly uniform ORMOSIL nanoparticles. In this process, the micelles or nanodroplets (nanoreactors) prepared in the microemulsion system provide surrounded cages for hydrolysis and condensation of ORMOSIL precursors. Because the size of particles is limited within the

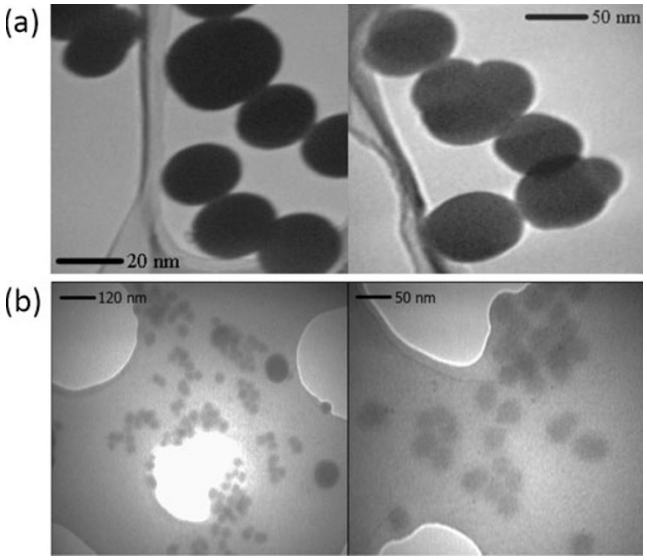

Fig. 2 TEM images of ORMOSIL nanoparticles synthesized using AOT (AOTORM NPs) (**a**), and ORMOSIL nanoparticles synthesized using Tween 80 (TWORM NPs) (**b**)

micelles, one of the most significant factors that controls the size and uniformity of the resulting particles is the volume of these self-assembled templates.

We found that one of the important factors determining the size distribution of the micelles and ORMOSIL nanoparticles is intrinsic properties of the surfactant especially solubility of the surfactant. The more water-soluble is the surfactant, the more monodisperse micelles and ORMOSIL nanoparticles can be achieved. Figure 3a shows the DLS result of AOT/water/DMSO micellar system; it is evident that low solubility of AOT surfactant has caused preparation of micelles with a wide variety of sizes from 200 to 900 nm. As a result of this polydisperse micellar system, the size of the nanoparticles (AOTORM) synthesized in the core of these micelles is relatively polydisperse (Figs. 2a and 3b).

However, because of the high solubility of Tween 80 in water, the micelles prepared in Tween 80/water/DMSO microemulsion are highly monodisperse with average hydrodynamic size of 11.7 nm (Fig. 3c) that have led to highly monodisperse nanoparticles with average hydrodynamic size of 10.9 nm (Fig. 3d).

To make the nanoparticles fluorescent, a hydrophobic fluorophore, Nile Red, was encapsulated into the silica matrix of AOTORM and TWORM. Since, Nile Red is not water-soluble, its molecules tend to nonpolar core of normal micelles. Once the condensation of ORMOSIL precursor, VTES, starts, the dye molecules are entrapped into ORMOSIL nanoparticles and will not be release. The average hydrodynamic size of the dye-doped particles was determined by DLS. It was seen that after entrapment of the dye, the size of the particles was increased from 35 to 53 nm for AOTORM nanoparticles and from 10.9 to 43 nm for TWORM nanoparticles that can confirm successful encapsulation of the dye (Fig. 4, Table 1).

To determine fluorescent properties of Nile Red after encapsulation of the organic dye within silica matrix, emission spectra of free Nile Red and Nile Red encapsulated in ORMOSIL nanoparticles were recorded by fluorescent spectroscopy. It was found that the excitation and emission wavelength of Nile Red doped in ORMOSIL nanoparticles were

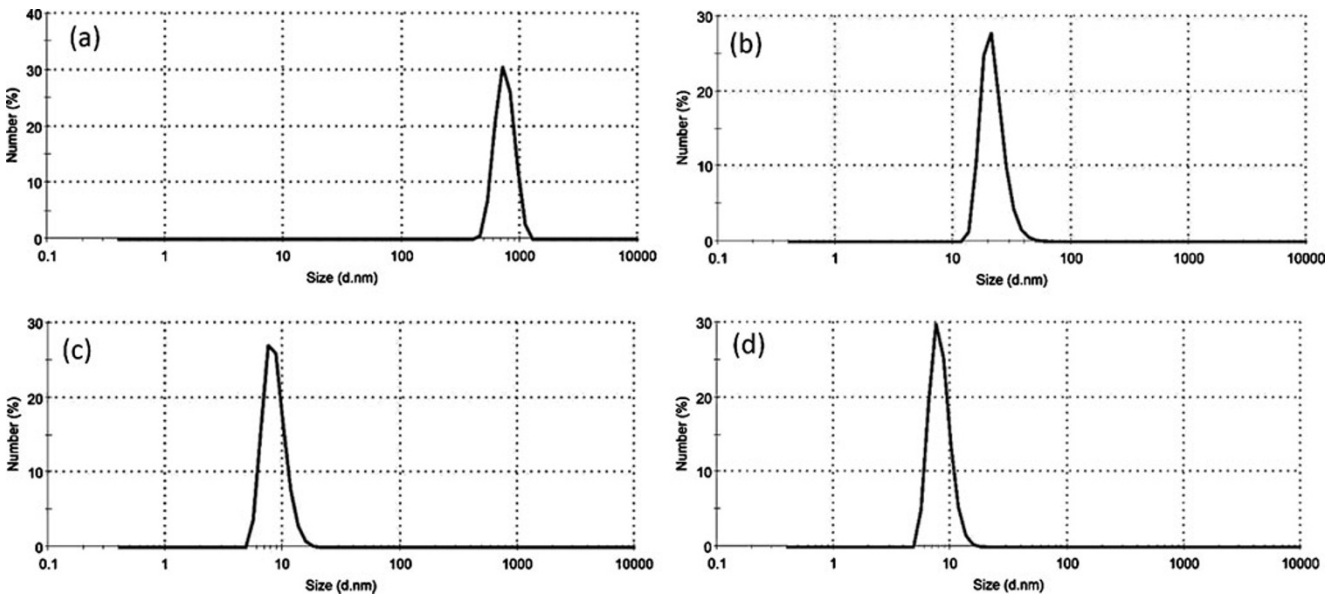

Fig. 3 Average hydrodynamic size distribution obtained by DLS from AOT micelles (**a**), AOTORM nanoparticles (**b**), Tween 80 micelles (**c**), and TWORM nanoparticles (**d**) with the mean size of 749, 35, 11.7, and 10.9 nm, respectively

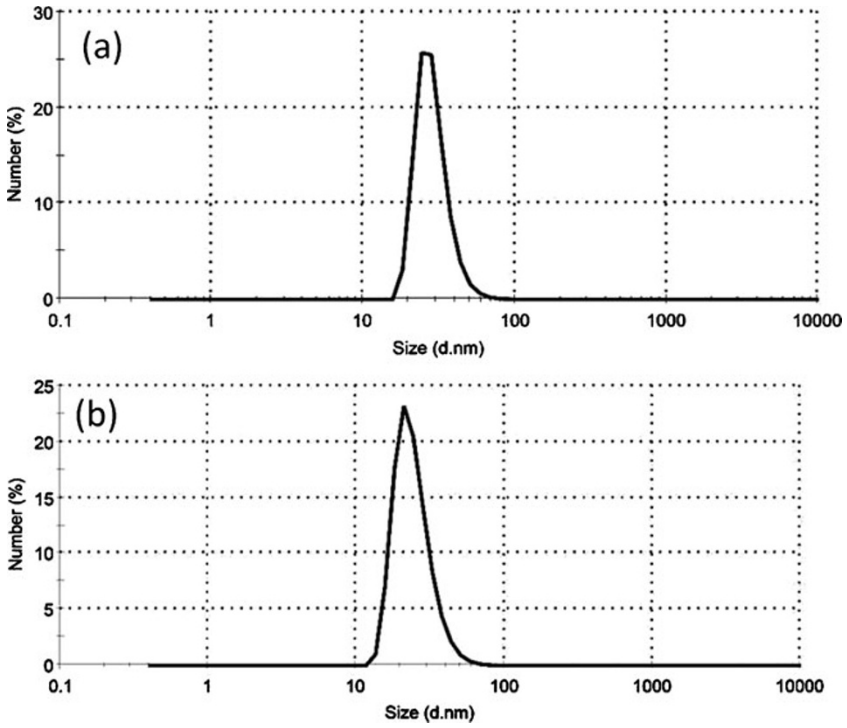

Fig. 4 Average hydrodynamic size distribution obtained by DLS from dye-doped AOTORM (**a**) and TWORM (**b**) nanoparticles with the mean size of 53 and 43 nm, respectively

570 and 640 nm, respectively, than are similar to the excitation and emission wavelength of free Nile Red (Fig. 5).

3.2 Effect of surfactant molecules on the surface charge of the particles

The surface properties and functionalization of silica nanoparticles play a critical role in biomedical applications. Based on DLVO theory, colloidal stability of the nanoparticles strongly depends on electrostatic charges and steric effects of the surface of nanoparticles (Ueno et al. 2008). The surface modification provides functional groups on the surface of silica nanoparticles that can be advantageous for their colloidal stability and can be applied for bioconjugation. Furthermore, surface functionalization of silica particles is important in their interaction with biological environments as well as their cellular uptake and cytotoxicity. The zeta potential (Z.P) of a particle is a representative of overall surface charge of the particle in the medium in which the particle is dispersed. The net charge at the nanoparticle surface is an accumulation of all charges present on the surface. There are various parameters that can affect Z.P of the nanoparticles such as presence of surfactant, connectivity of the solution, and pH (Bagwe et al. 2004; Wang et al. 2008). In terms of ORMOSIL nanoparticles, the factors that incorporate in overall charge are anionic silanol groups, cationic primary amine groups, and anionic or nonionic surfactant molecules. Silanol groups and surfactant molecules make the surface anionic while amine groups add cationic charges to the surface.

To demonstrate the impact of the presence of surfactant molecules on surface charge of ORMOSIL nanoparticles, we did a study of surface charge of the nanoparticles by Z.P measurements of AOTORM and TWORM nanoparticles. We used dialysis as a method for removing surfactant molecules gradually. Due to anionic hydrocarbon chains of AOT surfactant, the Z.P of AOT micelles is −44 mV. On the other hand, there is no ionic hydrocarbon chain in Tween 80; as a result, the Z.P of Tween 80 micelles is −4 mV (Fig. 6). Figure 7a, b shows Z.P of AOTORM and TWORM nanoparticles before dialysis (column 0) and after 2, 4, 6, and 8 days dialysis. AOTORM nanoparticles with no dialysis show Z.P of −89.9 mV (Fig. 7a), and Z.P of TWORM nanoparticles with no dialysis is −55 (Fig. 7b). Figure 7a, b shows a significant reduction in anionic charge of AOTORM and TWORM nanoparticles after 2 and 4 days dialysis. The amount of zeta potential for AOTORM NPs after 2, 4, 6, and 8 days dialysis is −57.2, −32.2, −23.3, and −21.5 mV, respectively, and for TWORM NPs after 2, 4, 6, and 8 days dialysis is, respectively, −3.7, −1.5, −1.2, and −1.1 mV.

Table 1 A comparisons of the size of ORMOSIL nanoparticles before and after the dye encapsulation

Particles	Hydrodynamic size before encapsulation (nm)	Hydrodynamic size after encapsulation (nm)
AOTORM	35	54
TWORM	10.9	43

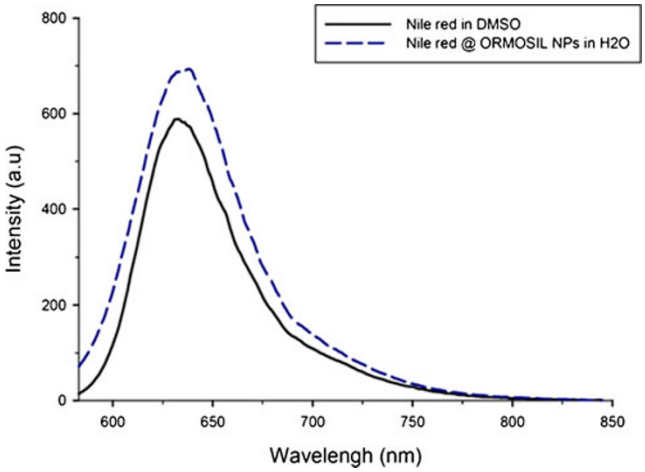

Fig. 5 Fluorescent spectrum of Nile Red dissolved in DMSO and Nile Red encapsulated in ORMOSIL nanoparticles

The reduction in both samples is mostly related to the reduction of surfactant molecules from the surface of the nanoparticles by dialysis. As dialysis continues, more surfactant molecules are removed which results in decreasing overall anionic charge of AOTORM nanoparticles. However, the efficacy of dialysis for removing remained AOT decreases after 4 days, and therefore, the overall charge of AOTORM nanoparticles remains constant in 6 and 8 days dialysis. This is the case for TWORM nanoparticles as well. It is evident that before removing the surfactant molecules completely, the surface charge of the nanoparticles is strongly dependent on the charges of surfactant molecules. By decreasing the number of surfactant molecules from the surface during dialysis, the zeta potential of the nanoparticles is changing from highly negative to less negative amount for AOT and less negative to positive amounts for Tween 80. The results reveal that the remained surfactant molecules have a very strong impact on the surface charge of nanoparticles and can cause a misunderstanding of actual charge of nanoparticles. In addition,

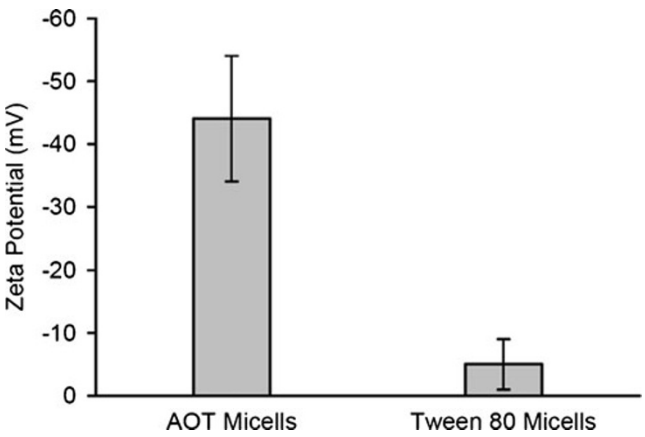

Fig. 6 The amount of zeta potential of AOT and Tween 80 micelles

data show that dialysis is an appropriate method to recover the nanoparticles from microemulsions effectively and effortlessly. All nanoparticles were dispersed in deionized water and all Z.Ps were measured at pH=8.

3.3 Active cell targeting

To make a nanoplatform for breast cancer specific targeting in vitro or in vivo, the nanoparticles must be conjugated with a biomoiety that recognizes these cells specifically. Among a number of crosslinker molecules, using the water-soluble carbodiimide EDC is a typical bioconjugation reaction to attach biomolecules to different particles. EDC provides covalent linkages between primary amines and carboxylic group. It activates the carboxyl groups of a carboxyl-containing molecule and forms an unstable intermediate compound that can be either hydrolyzed or linked with primary amines of an amine-containing molecule. This reaction leads to formation of stable amide bonds and can be followed for surface functionalization of nanoparticles (Sperling and Parak 2010).

Herein, we present the conjugation of ORMOSIL nanoparticles with Herceptin using EDC conjugation reaction. EDC was used to activate carboxylic group of Herceptin. This reaction leads to formation of Herceptin-functionalized ORMOSIL nanoparticles that enable to target HER2 receptors. Since SKBR3 human breast cancer cell line is a popular breast cancerous cell line with overexpression of HER2, it is an appropriate model to show active targeting by Herceptin-functionalized nanoparticles.

To confirm active targeting, we took fluorescent images of SKBR3 cells treated with various samples. In order to investigate the expression of HER2 receptor on the membrane of SKBR3 cells, we first added an appropriate concentration of Herceptin solution to the cells and then used a secondary antibody labeled with FITC (Sheep Anti Human IgG-FITC) against Herceptin for active staining of cell membrane of SKBR3 cells. Figure 8a shows that the cells treated with no sample have no autofluorescent. However, the cells that were treated with Herceptin as well as the secondary antibody labeled with FITC show strong green color emitted from FITC (Fig. 8b). These results confirm presence of HER2 receptor on the membrane of our cells. It is because Herceptin has made linkages to HE2 receptors and the secondary antibody has linked to Herceptin and stained the cells.

Figure 8c shows the images obtained from SKBR3 after treatment with dye-doped, amine-active, and non-conjugated TWORM NPs for 2 h. As seen in this image, the visible red fluorescence emitted from treated cells show that the cell membranes are stained with these particles that confirms nonspecific bandings between TWORM NPs and SKBR3 cell line. Figure 8e shows the florescent images

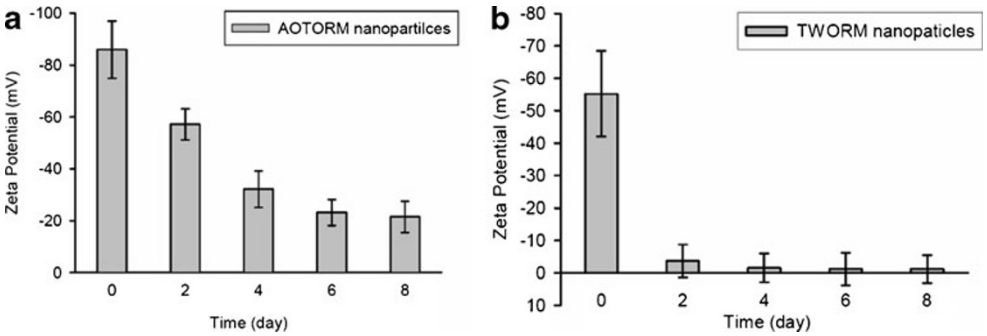

Fig. 7 The amount of zeta potential for AOTORM nanoparticles with no dialysis (column 0 day) and after 2, 4, 6, and 8 days dialysis (**a**), and the amount of zeta potential for TWORM nanoparticles with no dialysis (column 0 day) and after 2, 4, 6, and 8 days dialysis (**b**)

taken from the cells after being treated with dye-doped, amine-active, and non-conjugated AOTORM NPs for 2 h. The data confirm that there is no visible red fluorescence from the images of the cells treated with the dye-doped AOTORM NPs indicating that none of these particles has significant nonspecific bandings with the cell membranes.

In general, it is expected that amino-functionalized ORMOSIL nanoparticles have a tendency to go to the surface of the cells due to electrostatic interactions between positive charges, derived from positive amino groups on the surface of the nanoparticles, and negative charges of cell membrane. However, it should be noted that it is the overall

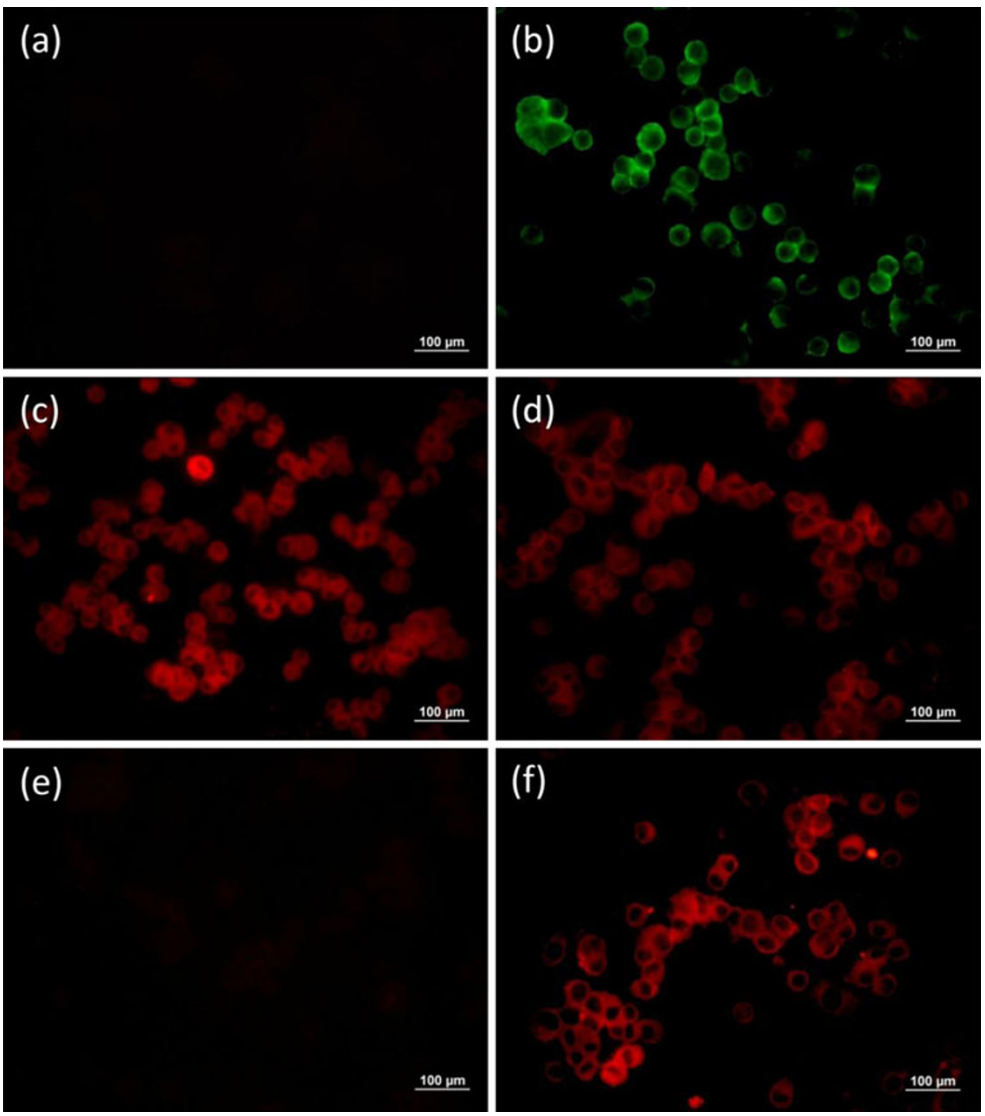

Fig. 8 Fluorescent images of SKBR3 cells treated with no sample (**a**), Herceptin and secondary antibody-FITC(**b**), dye-doped TWORM nanoparticles (**c**), dye-doped Herceptin-conjugated TWORM nanoparticles (**d**), dye-doped AOTORM nanoparticles (**e**), and dye-doped Herceptin-conjugated AOTORM nanoparticles (**f**)

surface charge of the nanoparticles that is mostly responsible for electrostatic interactions between the particles and the cell membrane. The overall surface charge of TWORM NPs is −3.7 mV and not so negative to prevent the formation of nonspecific bonding between these particles and the cell membranes. On the other hand, in terms of AOTORM NPs, the negative charges of remained AOT surfactant molecules and silanol groups on the surface of these nanoparticles shrink the efficiency of positive charges produced by amine groups and make the surface charge of these particles very negative, −57.2 mV. Therefore, by doing a simple washing by PBS buffer, most of the nonspecific bindings between the cell membrane and the nanoparticles can be removed. These results show that the intrinsic properties of surfactant used for synthesis of ORMOSIL NPs can have a critical role in electrostatic interactions between the surface of ORMOSIL NPs and the cell membrane.

Figure 8d, f, respectively, shows fluorescent microscopy images of SKBR3 cells stained with dye-doped TWORM and AOTORM nanoparticles both conjugated with Herceptin.

Figure 8d shows that the intensity of red fluorescent from the cells stained with Herceptin-conjugated TWORM NPs is similar to the cells stained with non-conjugated TWORM NPs. Tween 80 is not a dialyzable surfactant; therefore, it cannot be removed from the nanoparticles by short time dialysis which results in the existence of high concentration of surfactant on the surface of the particles that can produce many nonspecific interactions.

These surfactant molecules remained on the surface of TWORM nanoparticles can even prevent conjugation of primary amine groups of the nanoparticles with Herceptin; consequently, there is no significant difference between the stained cells with non-conjugated TWORM NPs and Herceptin-conjugated TWORM NPs.

Figure 8f shows the images taken from SKBR3 after treatment with dye-doped Herceptin-conjugated AOTORM NPs for 2 h. As seen in the images, in comparison to non-conjugated AOTORM NPs, there is strong visible red fluorescence from the images of the cells treated with conjugated AOTORM NPs that confirms significant specific targeting.

It can be seen that after 2 h of incubation with SKBR3, Herceptin-functionalized AOTORM NPs have produced strong specific bindings with extracellular domain of HER2 receptor on the cell membrane of SKBR3 that confirms efficient active targeting (Fig. 8f). It is evident that the functionalized nanoparticles are localized on the cell membrane by HER2 receptors.

In comparison to Tween 80, AOT is relatively removable by dialysis. As a result, after dialysis, most of the surfactant molecules used for synthesis of AOTORM NPs are removed that makes the surface of the particles appropriate for conjugation of Herceptin with amine groups and the negative chains of remained AOT molecules can be efficient to prevent strong nonspecific bandings.

Hence, we can conclude that the Herceptin-conjugated AOTORM NPs are able to distinguish and target HER2-positive cancerous cells from normal cells and therefore enable differentiation between HER2 normal and HER2 overexpressing human breast cancer cells in vitro. This application can be useful for determination of treatment method especially based on Herceptin targeting or other modalities. Moreover, our results show that the type of the surfactant used for formation of ORMOSIL NPs can play a significant role in interaction of the particles and the cell membrane.

4 Conclusion

Monodispersed ORMOSIL nanoparticles entrapped with a hydrophobic organic dye, Nile Red, were synthesized and characterized. In order to investigate the impact of the presence of surfactant molecules on the surface chemistry and surface charge of the nanoparticles, two different surfactants (AOT, Tween 80) were used as templates for formation of three different ORMOSIL nanoparticles. The results confirmed huge impact of these surfactants on the surface charge of the nanoparticles. Each of the nanoparticles had conjugated with Herceptin, to specific delivery of fluorescent nanoparticles to SKBR3 cells, as a model for HER2 overexpressing breast cancer. We found that the efficiency bioconjugation can be affected by presence of surfactant molecules on the surface of ORMOSIL nanoparticles. ORMOSIL nanoparticles conjugated with Herceptin are excellent candidates for determining whether breast cancer is HER2 positive or Her2 negative. This is important for determination of treatment strategy for breast cancer in clinics. Herceptin-functionalized ORMOSIL nanoparticles are also appropriate vehicles for targeted drug/gene delivery to breast cancer cells in the future works.

References

Bagwe RP, Yang C, Hilliard LR, Tan W (2004) Optimization of dye-doped silica nanoparticles prepared using a reverse microemulsion method. Langmuir 20(19):8336–8342

Bardhan R, Chen W, Perez Torres C, Bartels M, Huschka RM, Zhao LL, Morosan E, Pautler RG, Joshi A, Halas NJ (2009) Nanoshells with targeted simultaneous enhancement of magnetic and optical imaging and photothermal therapeutic response. Adv Funct Mater 19(24):3901–3909

Bharali D, Klejbor I, Stachowiak E, Dutta P, Roy I, Kaur N, Bergey E, Prasad P, Stachowiak M (2005) Organically modified silica nanoparticles: a nonviral vector for in vivo gene delivery and expression in the brain. Proc Natl Acad Sci U S A 102(32):11539

Byrne JD, Betancourt T, Brannon-Peppas L (2008) Active targeting schemes for nanoparticle systems in cancer therapeutics. Adv Drug Deliv Rev 60(15):1615–1626

Ciriminna R, Sciortino M, Alonzo G, Schrijver A, Pagliaro M (2011) From molecules to systems: sol-gel microencapsulation in silica-based materials. Chem Rev 111(2):765–789

Colombo M, Corsi F, Foschi D, Mazzantini E, Mazzucchelli S, Morasso C, Occhipinti E, Polito L, Prosperi D, Ronchi S (2010) HER2 targeting as a two-sided strategy for breast cancer diagnosis and treatment: Outlook and recent implications in nanomedical approaches. Pharmacol Res 62(2):150–165

Danhier F, Feron O, Préat V (2010) To exploit the tumor microenvironment: passive and active tumor targeting of nanocarriers for anti-cancer drug delivery. J Control Release 148(2):135–146

Darbandi M, Thomann R, Nann T (2005) Single quantum dots in silica spheres by microemulsion synthesis. Chem Mater 17(23):5720–5725

Gu FX, Karnik R, Wang AZ, Alexis F, Levy-Nissenbaum E, Hong S, Langer RS, Farokhzad OC (2007) Targeted nanoparticles for cancer therapy. Nano Today 2(3):14–21

Han Y, Jiang J, Lee SS, Ying JY (2008) Reverse microemulsion-mediated synthesis of silica-coated gold and silver nanoparticles. Langmuir 24(11):5842–5848

Harries M, Smith I (2002) The development and clinical use of trastuzumab (Herceptin). Endocr Relat Cancer 9(2):75

Hollamby MJ, Eastoe J, Chemelli A, Glatter O, Rogers S, Heenan RK, Grillo I (2009) Separation and purification of nanoparticles in a single step. Langmuir 26(10):6989–6994

Kim S, Ohulchanskyy T, Pudavar H, Pandey R, Prasad P (2007a) Organically modified silica nanoparticles co-encapsulating photosensitizing drug and aggregation-enhanced two-photon absorbing fluorescent dye aggregates for two-photon photodynamic therapy. J Am Chem Soc 129(9):2669–2675

Kim S, Pudavar H, Bonoiu A, Prasad P (2007b) Aggregation-enhanced fluorescence in organically modified silica nanoparticles: a novel approach toward high-signal-output nanoprobes for two-photon fluorescence bioimaging. Adv Mater 19(22):3791–3795

Kim S, Ohulchanskyy T, Bharali D, Chen Y, Pandey R, Prasad P (2009) Organically modified silica nanoparticles with intraparticle heavy-atom effect on the encapsulated photosensitizer for enhanced efficacy of photodynamic therapy. J Phys Chem C 113(29):12641–12644

Klejbor I, Stachowiak E, Bharali D, Roy I, Spodnik I, Morys J, Bergey E, Prasad P, Stachowiak M (2007) ORMOSIL nanoparticles as a non-viral gene delivery vector for modeling polyglutamine induced brain pathology. J Neurosci Methods 165(2):230–243

Kumar R, Roy I, Ohulchanskyy T, Goswami L, Bonoiu A, Bergey E, Tramposch K, Maitra A, Prasad P (2008) Covalently dye-linked, surface-controlled, and bioconjugated organically modified silica nanoparticles as targeted probes for optical imaging. Acs Nano 2(3):449–456

Kumar R, Roy I, Ohulchanskky T, Vathy L, Bergey E, Sajjad M, Prasad P (2010) In vivo biodistribution and clearance studies using multimodal organically modified silica nanoparticles. Acs Nano 4(2):699–708

Law W, Yong K, Roy I, Xu G, Ding H, Bergey E, Zeng H, Prasad P (2008) Optically and magnetically doped organically modified silica nanoparticles as efficient magnetically guided biomarkers for two-photon imaging of live cancer cells†. J Phys Chem C 112(21):7972–7977

Morishige T, Yoshioka Y, Inakura H, Tanabe A, Yao X, Narimatsu S, Monobe Y, Imazawa T, Tsunoda S, Tsutsumi Y (2010) The effect of surface modification of amorphous silica particles on NLRP3 inflammasome mediated IL-1 [beta] production, ROS production and endosomal rupture. Biomaterials 31(26):6833–6842

Nabeshi H, Yoshikawa T, Arimori A, Yoshida T, Tochigi S, Hirai T, Akase T, Nagano K, Abe Y, Kamada H (2011) Effect of surface properties of silica nanoparticles on their cytotoxicity and cellular distribution in murine macrophages. Nanoscale Res Lett 6(1):93

Nazar MF, Myakonkaya O, Shah SS, Eastoe J (2011) Separating nanoparticles from microemulsions. J Colloid Interface Sci 354(2):624–629

Nel AE, Mädler L, Velegol D, Xia T, Hoek EMV, Somasundaran P, Klaessig F, Castranova V, Thompson M (2009) Understanding biophysicochemical interactions at the nano–bio interface. Nat Mater 8(7):543–557

Ohulchanskyy TY, Roy I, Goswami LN, Chen Y, Bergey EJ, Pandey RK, Oseroff AR, Prasad PN (2007) Organically modified silica nanoparticles with covalently incorporated photosensitizer for photodynamic therapy of cancer. Nano Lett 7(9):2835–2842

Osseo-Asare K, Arriagada F (1990) Preparation of SiO_2 nanoparticles in a non-ionic reverse micellar system. Colloids Surf 50:321–339

Qian J, Li X, Wei M, Gao X, Xu Z, He S (2008) Bio-molecule-conjugated fluorescent organically modified silica nanoparticles as optical probes for cancer cell imaging. Opt Express 16(24):19568–19578

Qian J, Chen Q, Cai F, Kong S, Ho H, He S (2009) Quantum-dots-doped ORMOSIL nanoparticles as optical probes for total internal reflection fluorescence imaging of cancer cells. IEEE J Sel Top Quantum Electron 15(5):1374–1379

Qian J, Fu T, Zhan Q, He S (2010) Using some nanoparticles as contrast agents for optical bioimaging. IEEE J Sel Top Quantum Electron 16(3):672–684

Roy I, Ohulchanskyy T, Pudavar H, Bergey E, Oseroff A, Morgan J, Dougherty T, Prasad P (2003) Ceramic-based nanoparticles entrapping water-insoluble photosensitizing anticancer drugs: a novel drug- carrier system for photodynamic therapy. J Am Chem Soc 125(26):7860–7865

Salabat A, Eastoe J, Vesperinas A, Tabor RF, Mutch KJ (2008) Photorecovery of nanoparticles from an organic solvent. Langmuir 24(5):1829–1832

Slamon DJ, Clark GM, Wong SG, Levin WJ, Ullrich A, McGuire WL (1987) Human breast cancer: correlation of relapse and survival with amplification of the HER-2/neu oncogene. Science 235(4785):177–182

Slamon DJ, Leyland-Jones B, Shak S, Fuchs H, Paton V, Bajamonde A, Fleming T, Eiermann W, Wolter J, Pegram M, Baselga J, Norton L (2001) Use of chemotherapy plus a monoclonal antibody against HER2 for metastatic breast cancer that overexpresses HER2. N Engl J Med 344(11):783–792. doi:10.1056/NEJM200103153441101

Sperling R, Parak W (2010) Surface modification, functionalization and bioconjugation of colloidal inorganic nanoparticles. Philosophical transactions of the royal society a: mathematical. Phys Eng Sci 368 (1915):1333

Stober W, Fink A, Bohn E (1968) Controlled growth of monodisperse silica spheres in the micron size range. J Colloid Interface Sci 26(1):62–69

Sun X, Tabakman SM, Seo WS, Zhang L, Zhang G, Sherlock S, Bai L, Dai H (2009) Separation of nanoparticles in a density gradient: FeCo@ C and gold nanocrystals. Angew Chem 121(5):957–960

Ueno K, Inaba A, Kondoh M, Watanabe M (2008) Colloidal stability of bare and polymer-grafted silica nanoparticles in ionic liquids. Langmuir 24(10):5253–5259

Urata C, Aoyama Y, Tonegawa A, Yamauchi Y, Kuroda K (2009) Dialysis process for the removal of surfactants to form colloidal mesoporous silica nanoparticles. Chem Commun 34:5094–5096

Viswanathan K (2011) Preparation and characterization of fluorescent silica coated magnetic hybrid nanoparticles. Colloid Surface Physicochem Eng Aspect 386:11–15

Wang L, Zhao W, Tan W (2008) Bioconjugated silica nanoparticles: development and applications. Nano Res 1(2):99–115

Witton CJ, Reeves JR, Going JJ, Cooke TG, Bartlett J (2003) Expression of the HER1–4 family of receptor tyrosine kinases in breast cancer. J Pathol 200(3):290–297

Xia T, Kovochich M, Liong M, Meng H, Kabehie S, George S, Zink JI, Nel AE (2009) Polyethyleneimine coating enhances the cellular uptake of mesoporous silica nanoparticles and allows safe delivery of siRNA and DNA constructs. ACS Nano 3(10):3273–3286

Yong K, Roy I, Swihart M, Prasad P (2009) Multifunctional nanoparticles as biocompatible targeted probes for human cancer diagnosis and therapy. J Mater Chem 19:4655

Zhang R, Liu J, Han B, He J, Liu Z, Zhang J (2003) Recovery of nanoparticles from (EO) 8 (PO) 50 (EO) 8/p-xylene/H_2O microemulsions by tuning the temperature. Langmuir 19(21):8611–8614